Experimental evidence for Tayler instability in a liquid metal column

Martin Seilmayer, Frank Stefani,* Thomas Gundrum, Tom Weier, and Gunter Gerbeth
Helmholtz-Zentrum Dresden-Rossendorf, P.O. Box 510119, D-01314 Dresden, Germany

Marcus Gellert and Günther Rüdiger
Leibniz-Institut für Astrophysik Potsdam, An der Sternwarte 16, D-14482 Potsdam, Germany
(Dated: December 12, 2011)

In the current-driven, kink-type Tayler instability (TI) a sufficiently strong azimuthal magnetic field becomes unstable against non-axisymmetric perturbations. The TI has been discussed as a possible ingredient of the solar dynamo mechanism and a source of the helical structures in cosmic jets. It is also considered as a size limiting factor for liquid metal batteries. We report on a liquid metal TI experiment using a cylindrical column of the eutectic alloy GaInSn to which electrical currents of up to 8 kA are applied. We present results of external magnetic field measurements that indicate the occurrence of the TI in good agreement with numerical predictions. The interference of TI with the competing large scale convection, resulting from Joule heating, is also discussed.

The last years have seen a number of liquid metal experiments on various magnetohydrodynamic instabilities with relevance to the origin and the action of cosmic magnetic fields [1]. Dynamo action has been observed in the large scale liquid sodium experiments in Riga, Karlsruhe, and Cadarache [2]. The helical version of the magnetorotational instability (MRI) has been evidenced in the PROMISE experiment [3], and further experiments in Maryland [4] and Princeton [5] are devoted to the investigation of the standard version of MRI. What is missing yet in the liquid metal lab is any evidence of the Tayler instability (TI) [6]. This is in remarkable contrast to the vast experience in plasma physics where the (compressible) counterpart of TI is better known as the kink instability in a z-pinch [7], i.e. the limit of the Kruskal-Shafranov instability when the safety factor goes to zero. In astrophysics, TI has been discussed as a possible ingredient of an alternative, nonlinear stellar dynamo mechanism (Tayler-Spruit dynamo [8]), as a generation mechanism for helicity [9], and as a possible source of helical structures in galactic jets and outflows [10].

A particular motivation to study the TI in a liquid metal arises from the growing interest in large-scale liquid metal batteries as cheap means for the storage of highly intermittent renewable energies. Such a battery would consist of a self-assembling stratification of a heavy liquid half-metal (e.g. Bi, Sb) at the bottom, an appropriate molten salt as electrolyte in the middle, and a light alkaline or earth alkaline metal (e.g. Na, Mg) at the top. While small versions of this battery have already been tested [11], for larger versions the occurrence of TI could represent a serious problem for the integrity of the stratification. In a recent paper [12] we have proposed a simple trick to avoid the TI in liquid metal batteries by just returning the battery current through a bore in the middle. By the resulting change of the radial dependence of $B_\varphi(r)$ it is possible to prevent the condition for (ideal) TI, $\partial(rB_\varphi^2(r))/\partial r > 0$. Without such a provision, TI is expected to set in at some finite electrical current in the order of kA. The precise value is a fucntion of various material parameters, since for viscous and resistive fluids TI is known [13] to depend effectively on the Hartmann number $Ha = B_\varphi R(\sigma/(\rho\nu))^{1/2}$, where R is the radius of the column, σ the electrical conductivity, ρ the density, and ν the kinematic viscosity of the fluid.

In this paper, we present experimental results that confirm the numerically determined growth rates of TI [13]

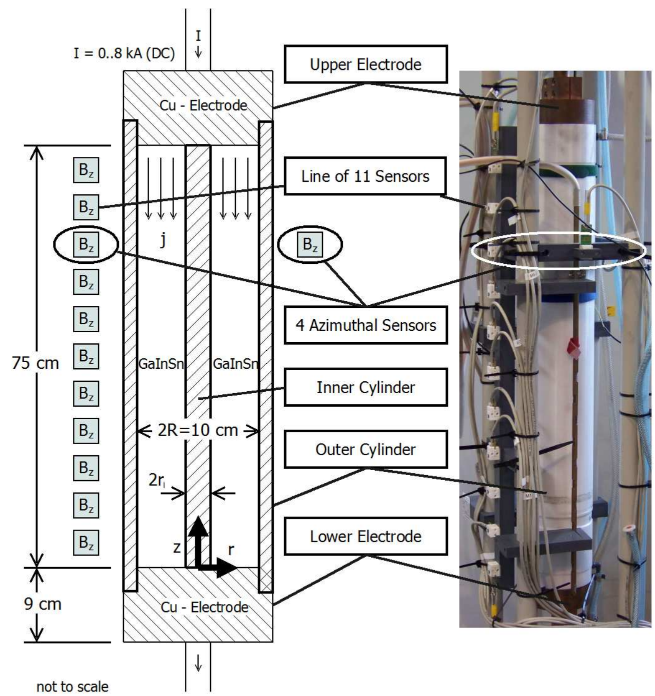

FIG. 1. Experimental set-up. Left: Scheme with liquid metal column and fluxgate sensors positioned along the vertical axis and the azimuth. Right: Photograph of the central part of the experiment.

* F.Stefani@hzdr.de

as well as the corresponding prediction that the critical current increases monotonically with the radius of an inner cylinder [12, 14].

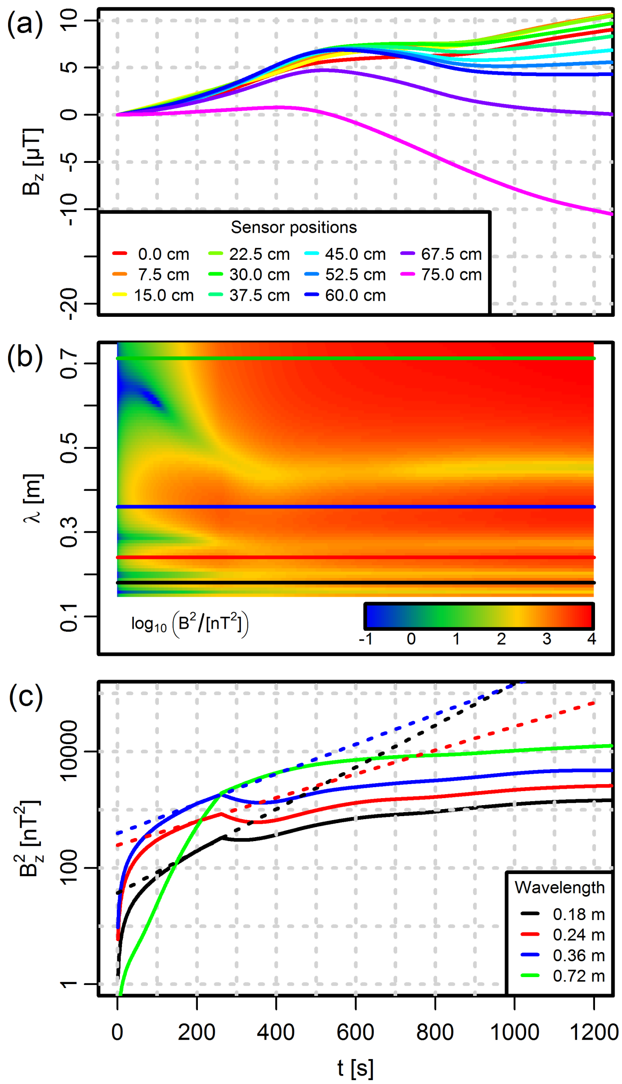

FIG. 2. Magnetic fields measured along the vertical axis, for r_i=12.5 mm and I=7 kA. (a) Time dependence of B_z at the 11 fluxgate sensors. (b) Power spectral density in dependence on time and wavelength. Note the dominance of short wavelength signals in the initial phase, and the dominance of the long wavelength signal at later times. (c) Detailed time evolution of the PSD for four significant wavelengths, showing a transition to an exponential growth around $t \sim$150 s, which is later stopped at $t \sim$280 s.

The central part of our TI experiment (Fig. 1) is an insulating cylinder of length 75 cm and inner diameter 10 cm, filled with the eutectic alloy GaInSn which is liquid at room temperatures. The physical properties of GaInSn at 25°C are: density $\rho = 6.36 \times 10^3$ kg/m^3, kinematic viscosity $\nu = 3.40 \times 10^{-7}$ m^2/s, electrical conductivity $\sigma = 3.27 \times 10^6\,(\Omega\,\mathrm{m})^{-1}$. At the top and bottom, the liquid metal column is contacted by two massive copper electrodes of height 9 cm which are connected by water cooled copper tubes to a DC power supply that is able to provide electrical currents of up to 8 kA. By intensively rubbing the GaInSn into the copper, we have provided a good wetting making the electrical contact as homogeneous as possible.

While in later experiments it is planned to use Ultrasonic Doppler Velocimetry (UDV) in order to measure directly the axial velocity component along the z-axis, for the first experiments we have decided not to use any inserts that could possibly disturb the homogeneous current going from the copper electrodes to the liquid. Therefore, for the identification of TI we exclusively rely on 14 external fluxgate sensors that measure the vertical component B_z of the magnetic field. Eleven of these sensors are aligned along the vertical axis (with a spacing of 7.5 cm), while the remaining three sensors are positioned along the azimuth in the upper part, approximately at 15 cm from the top electrode. The distance of the sensors from the outer rim of the liquid metal column is 7.5 cm. This rather large value, which is certainly not ideal to identify small wavelength perturbations, has been chosen in order to prevent any saturation effects of the fluxgate sensors in the comparably strong azimuthal field of the axial current.

The main goal of our experiment is to study the influence of the electric current through the fluid on the growth rate and on the amplitude of the magnetic field perturbations. This is done without any insert, as well as for two different radii of an inner non-conducting cylinder, r_i=6 mm and 12.5 mm, for which we expect a monotonic increase of the critical current.

For the particular case with r_i=12.5 mm and $I = 7$ kA, Figs. 2 and 3 illustrate the measured B_z data in dependence on the vertical position and on the azimuth, respectively, and the procedure of data analysis. In both cases, the time stamp and the field values were set to zero a few seconds after the switch-on process of the current had been finalized. Figure 2a shows the subsequent evolution of B_z measured at the 11 vertical positions. Most of the data in Fig. 2a show a collective long-term trend, whose source might be increasing convection, but possibly also some geometric changes (e.g. by thermal expansion of constructional parts) which could influence the projection of the strongly dominant azimuthal field component on the measured z-component.

Apart from this long term trend, the data of Fig. 2a contain much more details on the vertical dependence that can be extracted. For this purpose, we first subtract (at every time instant) the mean value and the linear trend in z-direction and compute then the Power Spectral Density (PSD) of the remaining signal. The resulting PSD, in dependence on time and wavelength, is shown in Fig. 2b. At the beginning we observe the simultaneous growth of three modes with short wavelengths, while later a long wavelength mode becomes dominant. The time dependencies of four exemplary modes with wavelengths 18 cm, 24 cm, 36 cm, and 72 cm are shown separately in

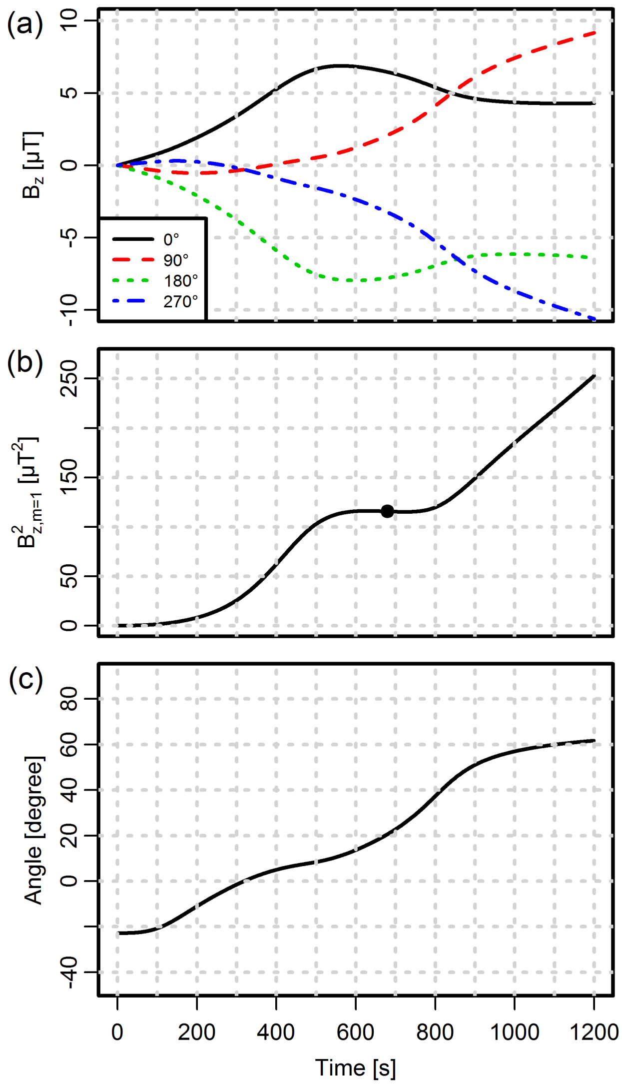

FIG. 3. Magnetic field data measured along the azimuth, for r_i=12.5 mm and I=7 kA. (a) Time dependence of B_z at the 4 fluxgate sensors. The m=1 character is clearly visible. (b) Squared magnetic field amplitude of the m=1 mode. (c) Angle of the m=1 mode.

Fig. 2c. Evidently, after some initial transient (lasting approximately until 150 s), the growth of all short wavelength modes acquires an exponential character, and we can read off the corresponding growth rates in the time interval between 200 s and 280 s (see the dotted lines in Fig. 2c). Note the similarity of the growth rates of the 18 cm and 36 cm mode which indicates the merging of next-neighbor cells (of the pure TI) as it is known from numerical simulations of the combined action of TI and (thermal) convection due to internal heating.

This regular exponential growth of the short wavelength modes stops suddenly at t=280 s, when the long wavelength mode (here with wavelength 72 cm) becomes dominant. Most interestingly, the growth rate of this

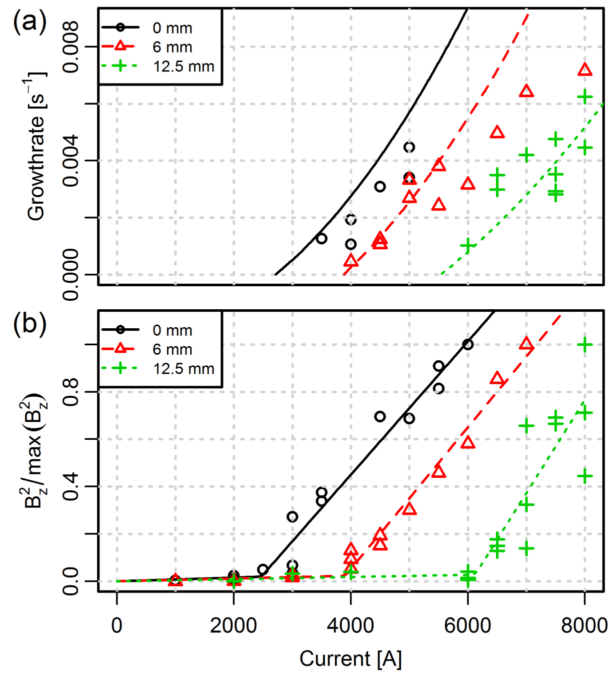

FIG. 4. (a) Measured growth rates and their numerical predictions for three different radii of the inner cylinder, in dependence on the current. (b) Measured squared magnetic field strength of the m=1 mode, and their piecewise linear fits. The maximum squared fields for r_i=0 mm, 6 mm, and 12.5 mm are 61.0 μT^2, 543.3 μT^2, and 1668.1 μT^2, respectively.

72 cm mode after the transition becomes quite similar to the growth rate of the 36 cm mode shortly before the transition. This may indicate a sudden doubling of the wavelength with increasing temperature and convection.

Now we turn to the discussion of the azimuthal dependence of the induced B_z-perturbations, as measured by the four sensors around the cylinder. The behaviour shown in Fig. 3a clearly indicates a non-axisymmetric (m=1) mode of the field with a growing amplitude at the beginning and some rotation and further growth at later times. The time evolution of the squared amplitude $(B_z(0°)-B_z(180°))^2+(B_z(90°)-B_z(270°))^2$ of this m=1 mode is presented in Fig. 3b, and its corresponding angle in Fig. 3c.

In Fig. 4 we compile the dependence of various quantities on the radius of the inner cylinder and on the current through the fluid. The growth rates of the 18 cm mode, as extracted from the periods with clear exponential growth (see Fig. 2c for one example), are compared with the numerically predicted growth rates in Fig. 4a. Despite some scatter of the data, we observe a quite reasonable agreement with the numerical predictions.

The second quantity of interest is the saturation level of the magnetic field. Similar to many other instabilities, for TI one would expect a more ore less linear behaviour of the saturated squared magnetic field above the critical current, according to $B^2 \sim (I-I_{\rm crit})$. However, the spe-

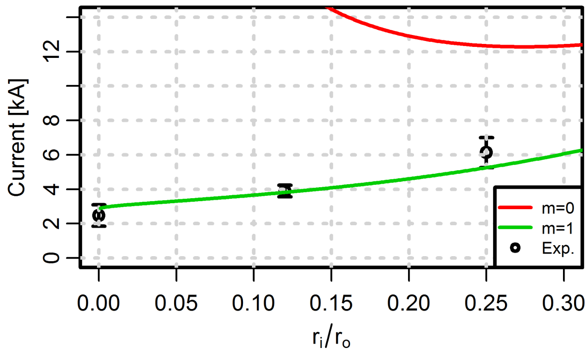

FIG. 5. Comparison of the determined critical currents with the numerical predictions for the m=1 mode. The numerical prediction for the m=0 (sausage) mode is indicated partly.

cific problem of our liquid metal experiment is that the saturation of the TI does not rely on an *intrinsic* back-reaction process, but on the *extrinsic* stabilizing effect of the increasing large scale convection. With this caveat in mind, in Fig. 4b we try to identify the critical current by plotting the squared magnetic field of the m=1 mode at the inflection point of the corresponding curves (indicated, for this example, by the point in Fig. 3b).

Starting at this inflection point we typically observe also a drift of the angle of the field pattern. We hypothesize that this "mode locking" starts when the long wavelength mode becomes dominant and aligns to some preferred azimuthal direction (determined, e.g., by slight geometric imperfections of the experimental set-up). The observed magnetic field level at this inflection point is thus yet determined by the TI alone. Insofar, it is reasonable to assume a monotonic, if not linear, dependence of the quadratic field strength (taken at the inflection point) on $(I - I_{\rm crit})$ to characterize the TI.

By applying a piecewise linear fit to the observed squared field intensities (see Fig. 4b), we can determine the critical current at the crossing point of the two straight lines. Figure 5 shows the critical currents determined that way and the error bars (with a 95 per cent confidence level), in comparison with the numerically determined ones. Despite the fact that the inflection-point criterion for the determination of the saturated magnetic field strength is certainly debatable, we obtain again a reasonable correspondence with the predicted critical currents.

The investigation of a current driven instability in a column of a liquid metal has revealed a rather complex behaviour, comprising (after some initial transient) an exponential growth of the anticipated TI mode followed by a large-scale convection dominated by Joule heating. From the sharp bends of the amplitude evolution of the short wavelength modes (see Fig. 2c) it becomes apparent that the growing intensity of convection limits the further growth of the TI. This is a drawback of the present experimental configuration, since it prevents any investigation of the *intrinsic* saturation mechanism of TI. The theoretical picture for this mechanism relies on the on-set of strong turbulence (due to the TI) leading to a radially dependent turbulent resistivity (β-effect, see [15]) which, in turn, would result in a modified radial current distribution that is just marginally stable against TI. The investigation of this interesting saturation mechanism would require a significant weakening of the role of Joule heating, either by choosing a horizontal orientation of the column (which, however, introduces an explicit symmetry breaking), or by an increase of the radius, and/or by the replacement of GaInSn with liquid sodium, for which TI is expected to occur already around 1 kA. Such a large scale sodium experiment, in which TI and MRI can be studied together, is planned for the future.

This work was supported by DFG in frame of SFB 609 and SPP 1488, and by the Energy Storage Initiative of the Helmholtz society. Fruitful discussions with Rainer Arlt, Rainer Hollerbach and Manfred Schultz are gratefully acknowledged. We thank Bernd Nowak und Thomas Wondrak for technical support.

[1] F. Stefani, A. Gailitis, and G. Gerbeth, ZAMM **88**, 930 (2008).
[2] A. Gailitis *et al.*, Phys. Rev. Lett. **84**, 4365 (2000); R. Stieglitz and U. Müller, Phys. Fluids **13**, 561 (2001); R. Monchaux et al., Phys. Rev. Lett. **98**, 044502 (2007).
[3] F. Stefani et al., Phys. Rev. Lett. **97**, 184502 (2006); F. Stefani et al., Phys. Rev. E **80**, 066303 (2009).
[4] D.R. Sisan, N. Mujica, W.A. Tillotson, Y.M. Huang, W. Dorland, A.B. Hassam, T.M. Antonsen, and D.P. Lathrop, Phys. Rev. Lett. **93**, 114502 (2004).
[5] M.D. Nornberg, H. Ji, E. Schartman, A. Roach, and J. Goodman, Phys. Rev. Lett. **104**, 074501 (2010).
[6] R.J. Tayler, MNRAS **161**, 365 (1973); Yu. V. Vandakurov, Sov. Astron. **16**, 265 (1972).
[7] W. L. Bergerson, Phys. Rev. Lett. **96**, 015004 (2006).
[8] H.C. Spruit, Astron. Astrophys. **381**, 923 (2002).
[9] M. Gellert, G. Rüdiger, and R. Hollerbach, MNRAS **414**, 2696 (2011).
[10] R. Moll, H.C. Spruit, M. Obergaulinger, Astron. Astrophys. **492**, 621 (2008).
[11] R.D. Weaver, S.W. Smith, and N.L. Willmann, J. Electrochem. Soc. **109**, 653 (1962); D.J. Bradwell, Liquid metal batteries: ambipolar electrolysis and alkaline earth electroalloying cells, PhD Thesis, MIT, 2011.
[12] F. Stefani, T. Weier, Th. Gundrum, and G. Gerbeth, Energy Conv. Manag. **52**, 2982 (2011).
[13] G. Rüdiger, M. Schultz, and M. Gellert, Astron. Nachr. **332** 17 (2011).
[14] G. Rüdiger and M. Schultz, Astron. Nachr. **331**, 121-129 (2010).
[15] M. Gellert, G. Rüdiger, Phys. Rev. E **80**, 046314 (2009).